

# A General Method for Assembling Single Colloidal Particle Lines

Jiaying Huang, Andrea R. Tao, Stephen Connor, Rongrui He, and Peidong Yang\*

*Department of Chemistry, University of California, Berkeley, Materials Science Division, Lawrence Berkeley National Laboratory, Berkeley, California 94720*

Received February 1, 2006

## ABSTRACT

We have developed a general method for assembling colloidal particles into one-dimensional lines of single particle thickness. Well-spaced, parallel single particle lines can be readily deposited on a substrate from a dilute Langmuir–Blodgett particle monolayer via a stick–slip motion of the water–substrate contact line. The particle density within the lines is controllable by the particle concentration in the monolayer as well as the pulling speed of the substrate. Lines of a great variety of materials and sizes, ranging from a few nanometers to a few micrometers, have been demonstrated. Multiple depositions create complex patterns such as cross lines, even of different particles. The ability of placing nanoparticles into one-dimensional arrays enables the construction of higher hierarchical device structures. For example, using gold nanoparticle seeds, vertical single nanowire arrays of silicon can be grown replicating the pattern of single particle lines.

Ordered colloidal particle arrays serve as a platform for developing nanoscale devices whose functionalities are enabled by the physical (i.e., optical, electrical, and magnetic) properties of the individual particles and their arrangement. For example, there has been increasing interest in one-dimensional (1D) nanoparticle arrays because they provide a model system to study transport phenomena<sup>1–3</sup> between nanoparticles in addition to their potential technological applications, such as chemical sensors<sup>4</sup> and lithography masks.<sup>5</sup> Current lithography methods can either directly produce nanoparticles in the form of arrays<sup>1,6</sup> or predefine a surface (geometrically, chemically, or electrostatically) to assist the assembly of nanoparticles.<sup>7–10</sup> Ordered arrangements of nanoparticles on templates such as block copolymer scaffolds<sup>11</sup> and along crystal step edges<sup>4,12</sup> have also been demonstrated. Here we report a facile, high throughput, lithography-free approach to create single colloidal particle lines employing the stick–slip motion of a water meniscus. Uniform 1D arrays of colloidal particles with sizes ranging from a few nanometers to a few micrometers can be readily produced with tunable particle density.

The design of the assembly method originates from a simple geometrical fact: two nonparallel planes always intersect in a line. When a substrate (the first plane) is dipped into a water-supported colloidal particle monolayer (the second plane), it intersects the monolayer with a contact line. From a geometrical point of view, this intersection is ideally a line with single particle thickness. To pull a single particle line out of the monolayer, intuitively, the following criteria should be met. First, the particle–substrate interaction at the

contact line should be favored over the interparticle interaction so that only the closest line of particles will be deposited. Second, a sharp contact angle between the monolayer and the substrate should be avoided. In a previous study, we discovered that when a completely wettable substrate (water contact angle  $<10^\circ$ ) is used to pull particles from such a monolayer, usually a continuous film of particles is obtained unless an appropriate amount of polymer is added into the water subphase to regulate the dewetting process, which leads to a fingering instability and consequently the deposition of ordered micrometer-scale particle stripes perpendicular to the meniscus.<sup>13</sup> The feature size of the obtained stripe patterns is usually in the range of a few to several tens of micrometers. Third, a discontinuous deposition mechanism is needed to avoid continuous deposition of lines one after another, which would be undistinguishable from a thin film. We have found that in a successful single particle line deposition, these criteria are met by using a dilute particle monolayer and a partially wettable substrate (i.e., hydrophobic).

The assembly process is illustrated in Figure 1a. First, colloidal particles are dispersed in an organic solvent such as chloroform or toluene. Then an appropriate amount of the dispersion is spread onto a water surface. When the solvent is evaporated, a Langmuir monolayer of the particles is obtained. Next, a substrate with a medium water contact angle (e.g., hydrofluoric acid-treated silicon wafer) is dipped into the monolayer. When the substrate is raised slowly with a motor, we observe a semiperiodic “stick and slip” motion of the contact line (see the Supporting Information, Video S1). The footprints of this stick–slip motion on the substrate are well-defined parallel lines of particles that are tens of micrometers apart. An optical microscopy (Nikon Optiphot,

\* Corresponding author. E-mail: p\_yang@berkeley.edu.

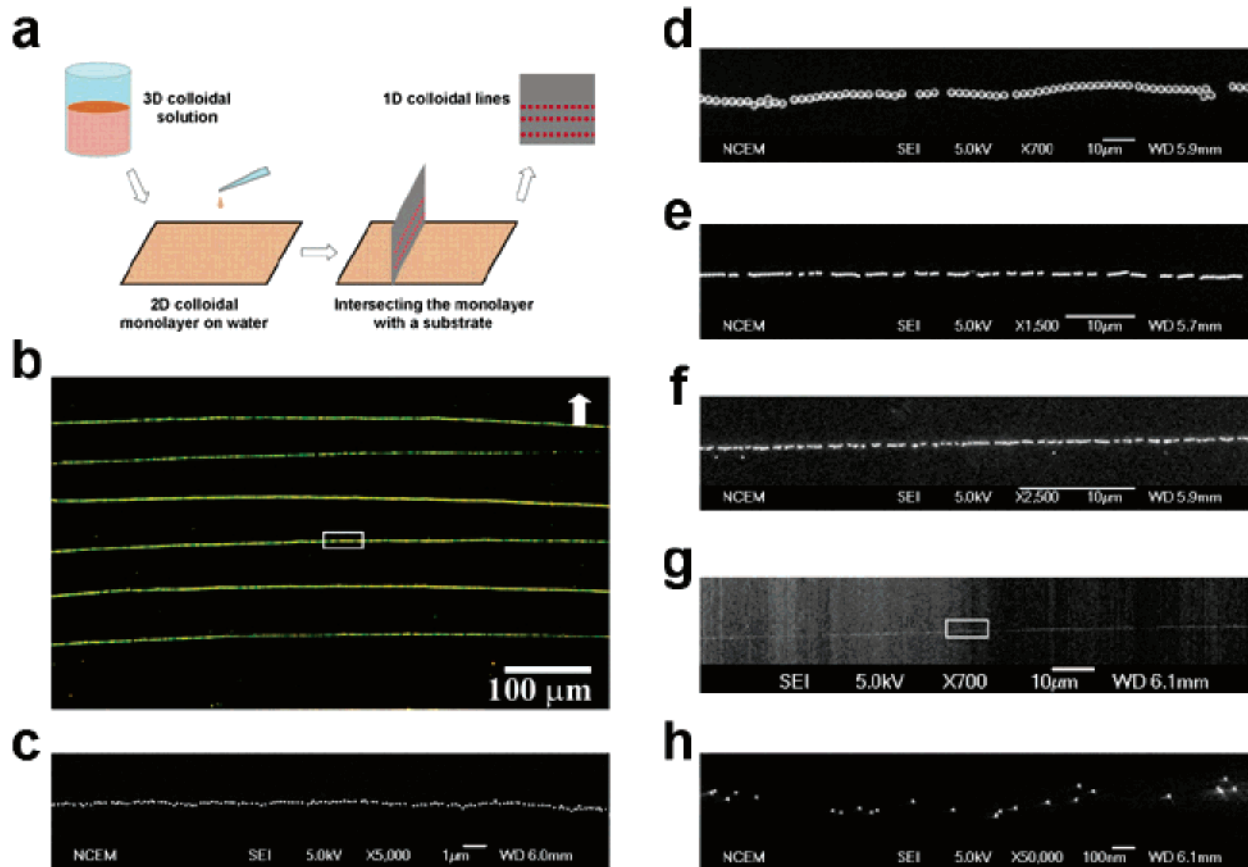


**Figure 1.** A general method for assembling 1D arrays of colloidal particles. (a) Schematic illustration showing colloidal particle dispersions with sequentially reduced dimensionality. First, a 3D colloidal solution is spread on to a water surface, forming a 2D particle monolayer. An immersed substrate intersects the monolayer and creates a contact line. Under proper conditions, parallel 1D arrays of particles can be deposited on the substrate upon lifting through a stick–slip motion of the contact line (see the Supporting Information, Video S1). A typical optical microscopy image of thus prepared Ag single nanocube (diameter  $\approx 50$  nm) lines on a Si substrate is shown in b. The curvature of the lines replicates that of the water meniscus. The typical line width is  $\sim 1$  nanoparticle as revealed by the scanning electron microscopy image in c. This method can readily produce 1D arrays of colloidal particles with a wide range of sizes and materials. A couple of examples are shown in the SEM images in (d)  $2.3 \mu\text{m}$ , (e)  $450$  nm, (f)  $160$  nm  $\text{SiO}_2$  spheres, and (g–h)  $7$  nm Pt nanoparticles. Part (h) is a higher magnification image showing the details of the Pt line in (g).

dark field mode) image of thus prepared silver nanoparticle lines is shown in Figure 1b. The line is about one nanoparticle thick ( $\sim 50$  nm) as revealed by scanning electron microscopy (SEM) (Figure 1c). The curvature of the lines is due to the shape of the meniscus. The line pattern extends over the entire substrate (typically at centimeter scale) and can be made within minutes. We have obtained uniform 1D arrays of particles with a great variety of sizes from a few micrometers to a few nanometers (Figure 1d–h). This is potentially a general technique for assembling colloidal particles.

The concept of contact-line deposition<sup>14–16</sup> and the stick–slip behavior of the meniscus<sup>17–20</sup> have been applied to deposit parallel particle bands on a vertical substrate from a colloidal particle dispersion. As the meniscus moves across the substrate, it can stick to the substrate and particles are deposited from solution. The interplay of pinning by the substrate and pinning by the particles determines the final pattern.<sup>14</sup> Dip-coating from a particle monolayer effectively eliminates pinning of the contact line by the predeposited particles from the dispersion, which would otherwise lead to multiparticle lines or even wide particle bands. Because

the contact line is only pinned by the substrate, single particle lines are collected. For the same reason, a monolayer of mixed particles (e.g.,  $2.3 \mu\text{m}$  silica and  $0.9 \mu\text{m}$  silica;  $80$  nm gold and  $7$  nm platinum) only produces lines with mixed particles, rather than separated lines of different particles (see the Supporting Information Figure S1). The main factors affecting the formation of single particle lines are the wettability of the substrate and the particle concentration in the monolayer. Low particle concentration in the monolayer, such as in the low surface pressure region ( $< 0.5$  mN/m) of the isotherm shown in Figure 2a, is a necessary condition for collecting lines with single-particle thickness. It is postulated that the interparticle interaction is weak, thus preventing the deposition of particle bands. We found that all of the substrates that can collect single particle lines have a water contact angle greater than  $20^\circ$ . These include acetone-cleaned silicon wafers with a thin native oxide layer (of a few nanometers) or a thick thermal oxide layer ( $\sim 50$  nm), hydrofluoric acid-cleaned silicon, and silanized glass slides. Completely wettable substrates (e.g., piranha-treated silicon substrates) are not suitable for obtaining single particle lines because water readily spreads over the substrate and the

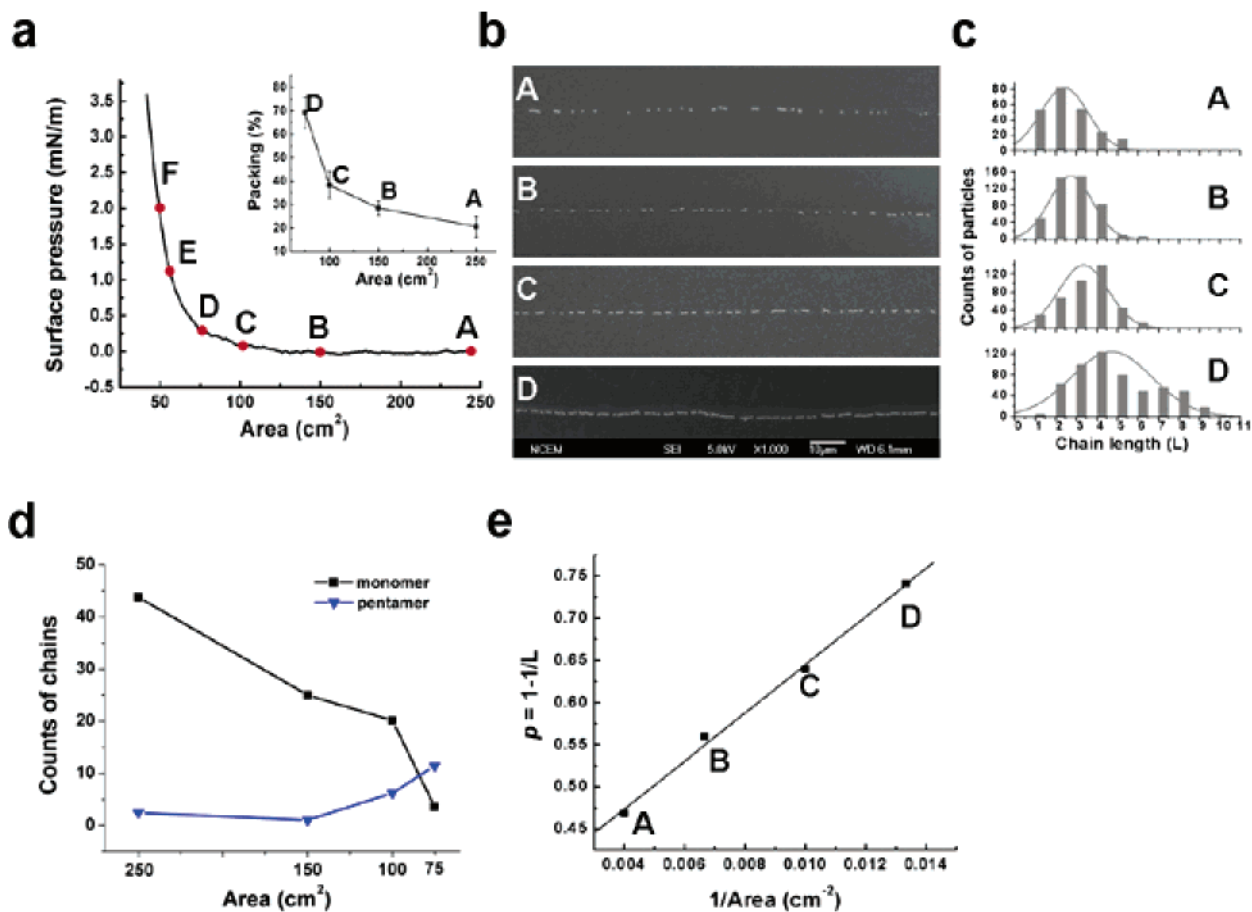


**Figure 2.** Particle density within the 1D arrays can be readily tuned by changing the particle concentration in the monolayer. (a) The isotherm of a monolayer of 450 nm SiO<sub>2</sub> spheres measured on a Langmuir–Blodgett trough. The film is compressed (from A, 250; B, 150; C, 100; to D, 75 cm<sup>2</sup>) to increase the particle concentration. As a result, the particle density in the resulting line pattern increases correspondingly (inset of a) as observed in the SEM images (b). (c) The length distribution of particle oligomers is also shifted to higher numbers. (d) At low particle concentration, monomers dominate (black squares). As the area of the monolayer decreases (i.e., particle concentration increases), the fraction of longer oligomers (e.g., pentamers) increases (blue triangles). Further compression leads to the deposition of branched lines (E, 60 cm<sup>2</sup>) before a continuous film (F, 50 cm<sup>2</sup>) is obtained (see the Supporting Information, Figure S2). (e) The probability of forming the colloidal particle oligomers is linearly dependent on the particle concentration in water.

contact line is not well-defined. In addition, the meniscus moves more smoothly and the stick–slip motion cannot be observed, resulting in a continuous film of particles. As we reported previously, if a small amount of water-soluble polymer is added into the water subphase, then a fingering instability of the contact line is developed during the rise of the substrate, which induces the deposition of ordered, vertical particle stripes with thicknesses of tens of micrometers on such hydrophilic substrates.<sup>13</sup>

The particle density within the lines can be conveniently tuned by changing the particle concentrations in the monolayer. Using a Langmuir–Blodgett trough, the monolayer can be controllably expanded or compressed by moving a barrier, thus changing the particle concentration.<sup>13,21–23</sup> A tensiometer equipped on the trough is used to monitor the surface pressure of the film during compression, yielding an isotherm plot (Figure 2a). Six depositions are performed at points A to F on the isotherm plot. Figure 2b shows typical SEM images of single particle lines of 450 nm silica spheres collected when the monolayer is sequentially compressed from point A to D at the same pulling speed (1 mm/min).

The increased particle concentration in the monolayer leads to increased packing density within the single particle lines (Figure 1a, inset). Meanwhile, as the film is compressed, silica spheres start to form particle “oligomers” in the collected lines (Figure 2b). As a result, the distribution of the chain lengths shifts to higher values (Figure 2c). As the particle concentration is increased, the number of particle “monomers” decreases significantly, whereas the number of longer chains, such as “pentamers” increases. This is due to the increased probability of particle chain growth at higher particle concentration. In an analogy to polymers, the average chain length of the colloidal particle oligomers ( $L$ ) can be calculated by the following formula.

$$L = \frac{\sum L_i n_i}{\sum n_i}$$

$L_i$  is the chain length, and  $n_i$  is the number of such chains. The calculated average lengths of the oligomers in single particle lines collected at points A to D are 1.88, 2.27, 2.77,

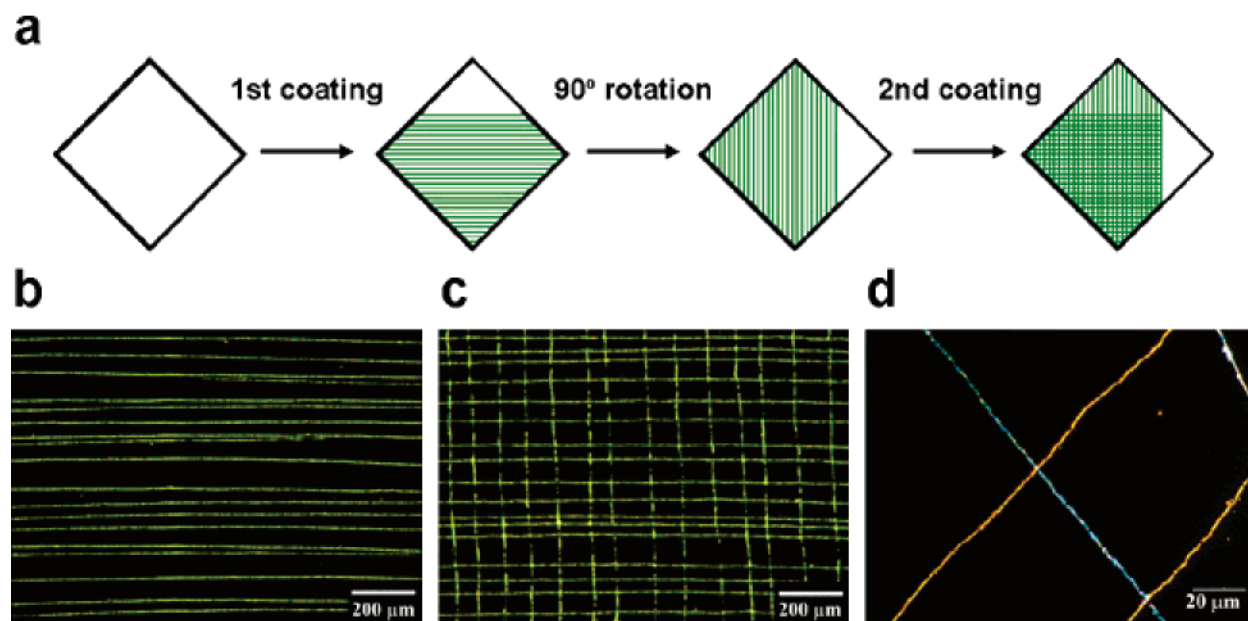


**Figure 3.** (a) Schematic diagrams illustrating the grid patterns obtained by two sequential crossed dip-coatings. Optical microscopy images showing (b) the Au single particle line pattern obtained by the first coating, (c) the grid pattern obtained by coating a second line pattern perpendicular to the first one, and (d) hybrid Au–Ag grid pattern by two dip-coating steps of Au and Ag nanoparticles, respectively.

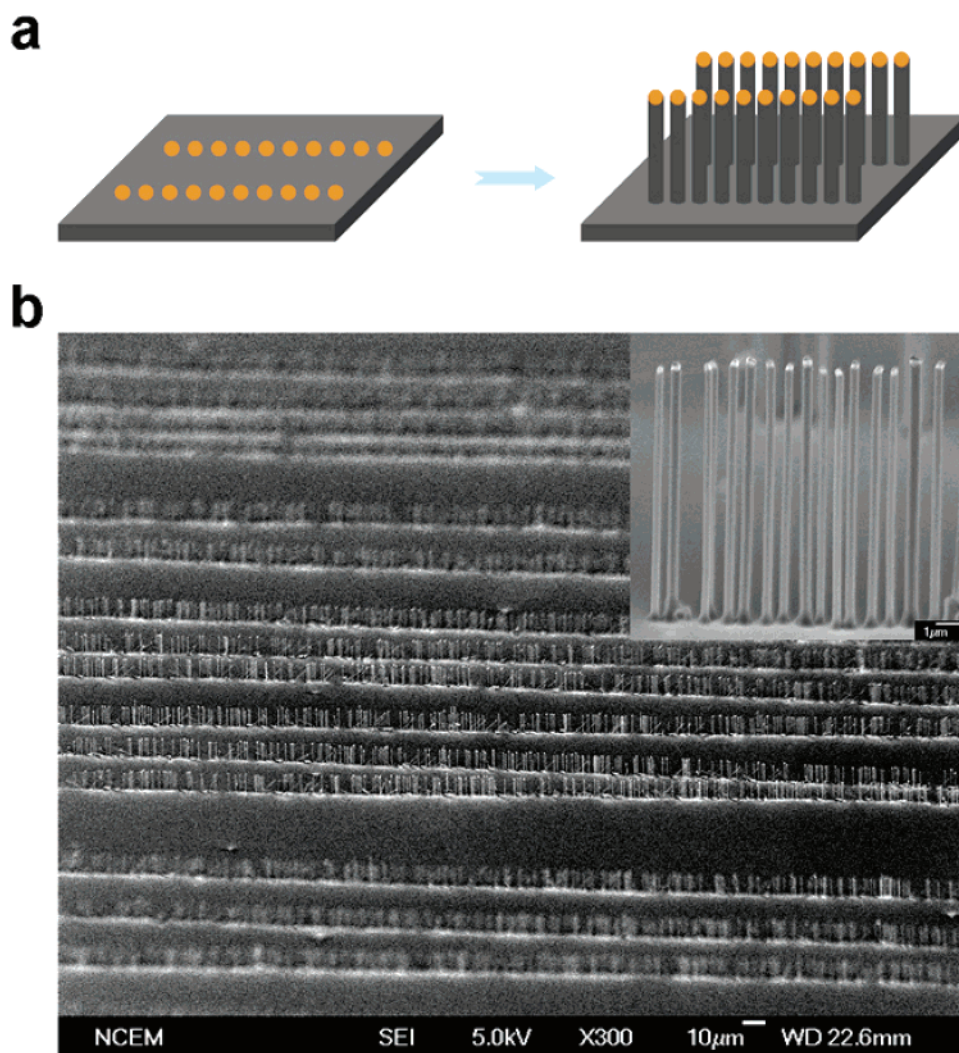


**Figure 4.** (a) 1D arrays of Si nanowires can be grown on the Au single nanoparticle lines, replicating the pattern of the Au nanoparticles. Part b and its inset are SEM images showing an overview and a close-up of the Si nanowire arrays, respectively.

and 3.86, respectively. Therefore, the probability of a monomer addition ( $p$ ) can be calculated accordingly by  $L = 1/(1 - p)$  (ref 24). By plotting the value of  $p$  against monolayer concentration ( $1/\text{area}$ ), a straight line is indeed obtained (Figure 2e). Upon further compression (E to F), branched and buckled lines, usually of a couple particles thick, are collected. Eventually, a continuous film is transferred to the substrate (see the Supporting Information, Figure S2).

Another way to change the particle density within the lines is to alter the sticking time of the contact line. At different pulling speeds, no obvious change in line spacing is observed, indicating that the sticking time of the meniscus is changed instead of its slipping distance. However, the particle density is not very sensitive to the pulling speed of the substrate. Within the available range of pulling speeds (1–40 mm/min) from the dipper on the Langmuir–Blodgett trough, one can prepare monomer-dominated single particle lines by using high pulling speeds (>20 mm/min). To obtain a higher packing density and longer particle oligomers, longer sticking times are needed. This could be achieved by using a slower motor, but slower pulling speeds (<1 mm/min) result in much extended deposition time. Therefore, a step pulling method is preferred. In this pulling mode, a substrate undergoes raise–stop–raise cycles. A longer sticking time can be readily achieved by increasing the length of the “stop” time from seconds to minutes. In this way, longer particle chains can be obtained, incorporating more than a hundred particles (see the Supporting Information, Figure S3).

A substrate with predeposited single particle lines can be dipped into the monolayer again to create a second pattern of parallel lines. Figure 3a shows the process of making crossed lines by two sequential depositions. The first set of parallel gold nanoparticle lines is deposited on a silicon wafer (Figure 3b), and then the substrate is rotated by 90° and dipped into the film again. The second set of gold lines overlaps with the first one, forming a grid pattern (Figure 3c). If the substrate is dipped into a monolayer of a different material, such as silver nanoparticles, then a hybrid cross pattern is obtained with gold and silver nanoparticle arrays perpendicular to each other. Figure 3d is a dark field optical microscopy image showing the hybrid gold (golden lines) and silver (bluish lines) grid pattern by two dip-coating steps of gold and silver nanoparticles on a glass slide. Because of the different plasmon response of the metal nanoparticles, their color contrast is evident. This should provide a useful device platform for investigating the electromagnetic coupling effect between metal nanoparticles.<sup>1,6,25,26</sup>

Our work reveals the versatility of the simple dip-coating process for aligning nanometer- to micrometer-sized objects. We would like to emphasize that existing nanoparticle patterning with comparable resolution always involves expensive lithography processing to a different extent. The striking simplicity of our dip-coating process may also attract theoretical investigation into the dewetting process of dilute particle monolayers. This facile dip-coating method for arranging nanoparticles into 1D arrays is robust and general. Essentially, the only limiting factor is the quality of the

particle monolayer. With the rich knowledge one can acquire from the colloidal particle processing chemistry,<sup>27</sup> this should be conveniently resolved for colloidal particles other than those mentioned here. The method we have developed here is an enabling technique that may lay the foundation for higher hierarchical device structures. For example, an immediate application for the gold single particle lines is in the growth of vertically aligned single silicon nanowire arrays. The one-dimensionality of the gold nanoparticle patterns can be readily transcribed into the final silicon nanowire arrays (Figure 4). This opens up the possibility of making large-scale nanoelectronic devices with individually addressable nanowire components, such as vertical field effect transistors (VFETs).

**Acknowledgment.** We thank S. Habas for preparing Pt nanoparticles and R. Fan, J. Goldberger and D. Sirbully for technical assistance and helpful discussions. This work was supported by the National Science Foundation (CAREER) and the Office of Basic Science, Department of Energy. J.H. gratefully acknowledges the Miller Institute for Basic Research in Science for a postdoc fellowship. A.R.T. gratefully acknowledges the National Science Foundation for a graduate research fellowship. S.C. gratefully acknowledges a summer research fellowship through Center of Integrated Nanomechanical Systems (COINS). We thank the National Center for Electron Microscopy for the use of their facilities.

**Supporting Information Available:** Methods and Materials; Video S1 and Figures S1–S3. This material is available free of charge via the Internet at <http://pubs.acs.org>.

## References

- (1) Maier, S. A.; Kik, P. G.; Atwater, H. A.; Meltzer, S.; Harel, E.; Koel, B. E.; Requicha, A. A. G. *Nat. Mater.* **2003**, *2*, 229–232.
- (2) Shipway, A. N.; Katz, E.; Willner, I. *ChemPhysChem* **2000**, *1*, 18–52.
- (3) Simon, U. *Adv. Mater.* **1998**, *10*, 1487–1492.
- (4) Favier, F.; Walter, E. C.; Zach, M. P.; Benter, T.; Penner, R. M. *Science* **2001**, *293*, 2227–2231.
- (5) Henrichs, S. E.; Sample, J. L.; Shiang, J. J.; Heath, J. R.; Collier, C. P.; Saykally, R. J. *J. Phys. Chem. B* **1999**, *103*, 3524–3528.
- (6) Wei, Q. H.; Su, K. H.; Durant, S.; Zhang, X. *Nano Lett.* **2004**, *4*, 1067–1071.
- (7) Barry, C. R.; Lwin, N. Z.; Zheng, W.; Jacobs, H. O. *Appl. Phys. Lett.* **2003**, *83*, 5527–5529.
- (8) Demers, L. M.; Ginger, D. S.; Park, S. J.; Li, Z.; Chung, S. W.; Mirkin, C. A. *Science* **2002**, *296*, 1836–1838.
- (9) Cui, Y.; Bjork, M. T.; Liddle, J. A.; Sonnichsen, C.; Boussert, B.; Alivisatos, A. P. *Nano Lett.* **2004**, *4*, 1093–1098.
- (10) Yin, Y.; Lu, Y.; Xia, Y. *J. Am. Chem. Soc.* **2001**, *123*, 771–772.
- (11) Lopes, W. A.; Jaeger, H. M. *Nature* **2001**, *414*, 735–738.
- (12) Zach, M. P.; Ng, K. H.; Penner, R. M. *Science* **2000**, *290*, 2120–2123.
- (13) Huang, J.; Kim, F.; Tao, A. R.; Connor, S.; Yang, P. *Nat. Mater.* **2005**, *4*, 896–900.
- (14) Deegan, R. D.; Bakajin, O.; Dupont, T. F.; Huber, G.; Nagel, S. R.; Witten, T. A. *Phys. Rev. E* **2000**, *62*, 756–765.
- (15) Deegan, R. D.; Bakajin, O.; Dupont, T. F.; Huber, G.; Nagel, S. R.; Witten, T. A. *Nature* **1997**, *389*, 827–829.
- (16) Govor, L. V.; Reiter, G.; Parisi, J.; Bauer, G. H. *Phys. Rev. E* **2004**, *69*, 061609.
- (17) Gleiche, M.; Chi, L. F.; Fuchs, H. *Nature* **2000**, *403*, 173–175.
- (18) Kovalchuk, V. I.; Bondarenko, M. P.; Zholkovskiy, E. K.; Vollhardt, A. *J. Phys. Chem. B* **2003**, *107*, 3486–3495.

- (19) Giraldo, O.; Durand, J. P.; Ramanan, H.; Laubernds, K.; Suib, S. L.; Tsapatsis, M.; Brock, S. L.; Marquez, M. *Angew. Chem., Int. Ed.* **2003**, *42*, 2905–2909.
- (20) Diao, J. J.; Sun, J. W.; Hutchison, J. B.; Reeves, M. E. *Appl. Phys. Lett.* **2005**, *87*, 103113.
- (21) Roberts, G. *Langmuir—Blodgett Films*; Plenum: New York, 1990; p 425.
- (22) Collier, C. P.; Saykally, R. J.; Shiang, J. J.; Henrichs, S. E.; Heath, J. R. *Science* **1997**, *277*, 1978–1981.
- (23) Kim, F.; Kwan, S.; Akana, J.; Yang, P. *J. Am. Chem. Soc.* **2001**, *123*, 4360–4361.
- (24) Bromberg, S.; Dill, K. A. *Molecular Driving Forces: Statistical Thermodynamics in Chemistry & Biology*; Garland Publishing: New York, 2002; p 686.
- (25) Reinhard, B. M.; Siu, M.; Agarwal, H.; Alivisatos, A. P.; Liphardt, J. *Nano Lett.* **2005**, *5*, 2246–2252.
- (26) Sonnichsen, C.; Reinhard, B. M.; Liphardt, J.; Alivisatos, A. P. *Nat. Biotechnol.* **2005**, *23*, 741–745.
- (27) Ross, S.; Morrison, I. D. *Colloidal Systems and Interfaces*; Wiley-Interscience: New York, 1988.

NL060235U